

# Thermochromism, the Alexandrite Effect, and Dynamic Jahn–Teller Distortions in $\text{Ho}_2\text{Cu}(\text{TeO}_3)_2(\text{SO}_4)_2$

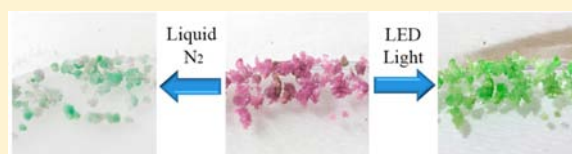
Jian Lin,<sup>†,‡</sup> Kariem Diefenbach,<sup>†</sup> Justin N. Cross,<sup>†,‡</sup> Jean-Marie Babo,<sup>‡</sup> and Thomas E. Albrecht-Schmitt<sup>\*,†</sup>

<sup>†</sup>Department of Chemistry and Biochemistry, Florida State University, 95 Chieftan Way, 310 DLC, Tallahassee, Florida 32306, United States

<sup>‡</sup>Department of Civil & Environmental Engineering & Earth Sciences, University of Notre Dame, 156 Fitzpatrick Hall, Notre Dame, Indiana, 46556, United States

## Supporting Information

**ABSTRACT:** A 3d–4f heterobimetallic material with mixed anions,  $\text{Ho}_2\text{Cu}(\text{TeO}_3)_2(\text{SO}_4)_2$ , has been prepared under hydrothermal conditions.  $\text{Ho}_2\text{Cu}(\text{TeO}_3)_2(\text{SO}_4)_2$  exhibits both thermochromism and the Alexandrite effect. Variable temperature single crystal X-ray diffraction and UV–vis–NIR spectroscopy reveal that changes in the  $\text{Cu}^{\text{II}}$  coordination geometry result in negative thermal expansion of axial Cu–O bonds that plays a role in the thermochromic transition of  $\text{Ho}_2\text{Cu}(\text{TeO}_3)_2(\text{SO}_4)_2$ . Magnetic studies reveal an effective magnetic moment of 14.97  $\mu\text{B}$ , which has a good agreement with the calculated value of 15.09  $\mu\text{B}$ .



## INTRODUCTION

Hetero-bimetallic materials display numerous functions that include single molecule magnetism, selective ion-exchange, gas storage, fluorescence, and optical sensing.<sup>1</sup> The incorporation of lanthanides into these compounds can provide both large magnetic moments and considerable single ion anisotropy.<sup>2</sup> The optical properties of lanthanide ions such as luminescence and the Alexandrite effect allow one to couple optical and magnetic properties.<sup>3</sup> The inclusion of a transition metal enriches these materials to include electronic conductivity, ferromagnetism, and thermochromism.<sup>4</sup> The preparation of these 3d–4f heterobimetallic materials can be quite challenging owing to complexation competitions between 3d and 4f metals with the ligands, which typically results in the formation of multiple homometallic products rather than a single heterobimetallic complex.<sup>1a</sup> The majority of 3d–4f compounds have been synthesized using organic linkers such as carboxylates and phosphonates.<sup>1c–f,4e,5</sup> While this class of metal–organic frameworks (MOFs) is promising in many regards, they tend to be of relatively low thermal stability and are vulnerable to decomposition. Purely inorganic 3d–4f heterometallic materials are still rare.<sup>6</sup> Herein we report on a new hetero-bimetallic mixed anion material,  $\text{Ho}_2\text{Cu}(\text{TeO}_3)_2(\text{SO}_4)_2$ , that displays both remarkable structural complexity and a host of atypical electronic properties.

We have recently undertaken a study of the materials chemistry of an array of d- and f-block tellurites because of the propensity of these materials to exhibit unusual bonding that gives rise to key properties such as guest–host chemistry.<sup>7</sup> Tellurites possess a stereochemically active lone-pair of electrons on  $\text{Te}^{\text{IV}}$ , and these anions can be interconnected to form polymeric structures, which results in highly variable coordination environments in this family of compounds.<sup>8</sup> We present here a method for preparing a holmium copper tellurite

sulfate,  $\text{Ho}_2\text{Cu}(\text{TeO}_3)_2(\text{SO}_4)_2$ .<sup>9</sup> To the best of our knowledge, this is one of the few examples of inorganic 3d–4f bimetallic compounds containing mixed anions.  $\text{Ho}_2\text{Cu}(\text{TeO}_3)_2(\text{SO}_4)_2$  shows both thermochromic and Alexandrite effects. Thermochromism is the reversible change in the color of a compound when subjected to a temperature variation within a certain range; substances with the Alexandrite effect change color under variable lighting sources.<sup>10</sup>  $\text{Ho}_2\text{Cu}(\text{TeO}_3)_2(\text{SO}_4)_2$  is one of the rare materials that exhibits both of these properties.

## RESULTS AND DISCUSSION

Single crystal X-ray diffraction reveals that  $\text{Ho}_2\text{Cu}(\text{TeO}_3)_2(\text{SO}_4)_2$  crystallizes in the triclinic space group  $P\bar{1}$  with a three-dimensional (3D) framework (cf. Table S1, Supporting Information). As shown in Figure 1a, the  $\text{TeO}_3^{2-}$  and  $\text{SO}_4^{2-}$  ligands both chelate and bridge the  $\text{Ho}^{\text{III}}$  and  $\text{Cu}^{\text{II}}$  ions. Each  $\text{Ho}^{\text{III}}$  is bound to three  $\text{TeO}_3^{2-}$  anions and three  $\text{SO}_4^{2-}$  anions. The  $\text{Ho}^{\text{III}}$  polyhedra edge-share with two other  $\text{Ho}^{\text{III}}$  centers and one  $\text{Cu}^{\text{II}}$  center. The  $\text{Ho}^{\text{III}}$  ions edge-share alternatively, forming one-dimensional (1D) Ho–oxo ribbons extending along the  $b$  axis (cf. Figure S1, Supporting Information). Lanthanides are typically 8-, 9-, or 10-coordinate when bound by oxygen atoms, yielding different coordination geometries based on square antiprisms, dodecahedra, tricapped trigonal prisms, capped triangular cupola, etc.<sup>11</sup> Shape8 calculations demonstrate that the geometry for the  $\text{HoO}_8$  unit is best described as a distorted trigonal dodecahedron with approximate  $D_{2d}$  symmetry (cf. Figure 1b).<sup>12</sup> The Ho–O bond distances range from 2.269(4) to 2.510(4) Å at 100 K (cf. Table S2, Supporting Information). The  $\text{Cu}^{\text{II}}$  ions are in a distorted octahedral geometry. The six O atoms bound to  $\text{Cu}^{\text{II}}$

Received: September 25, 2013

Published: November 1, 2013

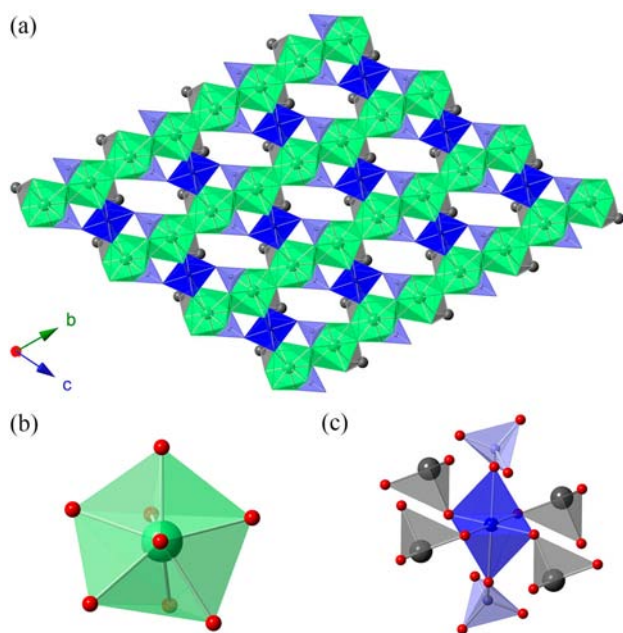


**Figure 1.** (a) View of the structure of  $\text{Ho}_2\text{Cu}(\text{TeO}_3)_2(\text{SO}_4)_2$  extending along the  $a$  axis. (b) Representation of the trigonal dodecahedral coordination environment of  $\text{Ho}^{\text{III}}$ . (c)  $[\text{Cu}(\text{TeO}_3)_2(\text{SO}_4)_2]^{6-}$  unit. Ho polyhedra are shown in green, Cu polyhedra are in dark blue,  $\text{TeO}_3$  polyhedra are in gray,  $\text{SO}_4$  tetrahedra are in purple, and O atoms are in red.

are donated from four  $\text{TeO}_3^{2-}$  anions, which are the equatorial O atoms, and two  $\text{SO}_4^{2-}$  anions, which are the axial O atoms, forming a  $[\text{Cu}(\text{TeO}_3)_2(\text{SO}_4)_2]^{6-}$  unit (cf. Figure 1c).

The reversible thermochromic transition of  $\text{Ho}_2\text{Cu}(\text{TeO}_3)_2(\text{SO}_4)_2$  is revealed by dipping the crystals into liquid nitrogen (cf. video in Supporting Information). Under standard room fluorescence lighting,  $\text{Ho}_2\text{Cu}(\text{TeO}_3)_2(\text{SO}_4)_2$  crystals are pink at 298 K which is typical for Ho compounds (Figure 2b).<sup>3c</sup>

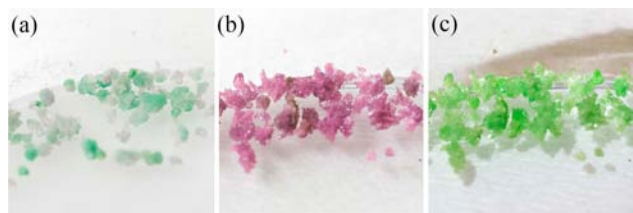


**Figure 2.** Photographs of  $\text{Ho}_2\text{Cu}(\text{TeO}_3)_2(\text{SO}_4)_2$  crystals showing the thermochromic and Alexandrite effects. (a) Under standard fluorescent light at 100 K, (b) under standard fluorescent light at 298 K, (c) under LED light at 298 K.

When the temperature decreases approximately to 100 K, the crystals change to a green hue due to contributions from the  $\text{Cu}^{\text{II}}$  ions (Figure 2a). The pink color is recovered when the sample is returned to room temperature. The color change of  $\text{Ho}_2\text{Cu}(\text{TeO}_3)_2(\text{SO}_4)_2$  can also be achieved by changing the light source used for illumination. Specifically, the sample appears pink under standard fluorescence lighting, while it appears green under natural light, a halogen or LED lamp at room temperature (Figure 2c). This phenomenon is referred to as the Alexandrite effect.

Thermochromism can be attributed to a variety of mechanisms such as phase changes,<sup>4d,13</sup> a change in the

coordination geometry of the transition metal,<sup>4c</sup> alterations of the excited states in thermal equilibrium,<sup>14</sup> and a change of electron configuration in spin-crossover complexes.<sup>15</sup> In our scenario, the change of the  $\text{Cu}^{\text{II}}$  coordination geometry contributes to the thermochromic transition. The thermal-driven change of the  $\text{Cu}^{\text{II}}$  geometry is determined by X-ray crystal structure analyses at two different temperatures (298 K and 100 K). Cu and O atoms show more significant thermal vibrations at 298 K as shown by the larger ellipsoids in Figure 3.

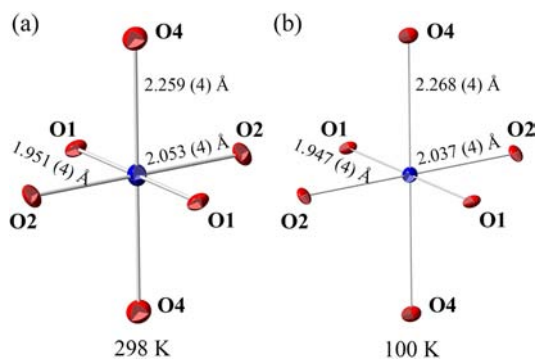


**Figure 3.** (a, b) ORTEP (50% probability level ellipsoids) representations of copper octahedra showing the changes of the  $\text{Cu}^{\text{II}}$ -O bond lengths, driven by a more pronounced Jahn-Teller effect at 100 K.

The  $\text{Cu}^{\text{II}}$  ions lie on an inversion center and are coordinated by three crystallographically independent O atoms. At 100 K, the Cu-O bond lengths in the equatorial plane decrease from 1.951(4) Å to 1.947(4) Å for  $\text{O}_1$  and from 2.053(4) Å to 2.037(4) Å for  $\text{O}_2$ , respectively. The axial Cu-O<sub>4</sub> bond length, however, increases from 2.259(4) Å to 2.268(4) Å. By the application of temperature or pressure, the nature of a Jahn-Teller distortion can be manipulated as exhibited here, where the geometry shifts more toward a square planar environment.<sup>16</sup> Lowering the temperature leads to a more pronounced Jahn-Teller distortion in the  $\text{Cu}^{\text{II}}$  environment, leading to the color change of  $\text{Ho}_2\text{Cu}(\text{TeO}_3)_2(\text{SO}_4)_2$ . A similar effect has been observed in  $[\text{Cu}(\text{bpym})-(\text{tcnoet})_2]\cdot\text{H}_2\text{O}$  (tcnoet = 1,1,3,3-tetracyano-2-ethoxypropene anion; bpym = 2,2'-bipyrimidine).<sup>4d</sup>

Variable temperature UV-vis-NIR absorption spectra were acquired from single crystals using a microspectrophotometer. Crystals were placed on quartz slides under Krytox oil, and the data were collected from 200 to 900 nm. As shown in Figure 4,  $\text{Ho}_2\text{Cu}(\text{TeO}_3)_2(\text{SO}_4)_2$  has a broad absorbance from approximately 600 to 900 nm, which can be assigned to a combination of ligand-to- $\text{Cu}^{\text{II}}$  charge transfer and d-d transitions of  $\text{Cu}^{\text{II}}$  ions.<sup>17</sup> The sharp f-f electronic transitions of  $\text{Ho}^{\text{III}}$  have been assigned, and the signature peaks are displayed in the spectra.<sup>18</sup> There are only very subtle changes between the spectrum at 298 K and spectra acquired at lower temperatures. While it is true that the coordination environment of the  $\text{Cu}^{\text{II}}$  ions is changing, the sharpness and intensity of the  $\text{Ho}^{\text{III}}$  transitions are also altered by the varying temperature as well. The  $\text{Ho}^{\text{III}}\ ^5\text{I}_8 \rightarrow\ ^5\text{F}_5$  transition at 650 nm is the most affected. It appears that unlike in most thermochromic materials where distortions of a single metal ion are responsible for the colors changes, in  $\text{Ho}_2\text{Cu}(\text{TeO}_3)_2(\text{SO}_4)_2$  there is a subtle interplay between the absorption features of the two different metal ions. In fact, if one were to only have the spectra in hand, a color change might

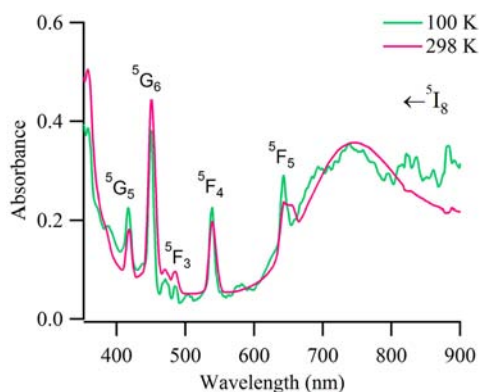


**Figure 4.** UV-vis spectra of  $\text{Ho}_2\text{Cu}(\text{TeO}_3)_2(\text{SO}_4)_2$  at 100 K and at 298 K.

not be anticipated at all, but one is clearly observed by the naked eye, much like the Alexandrite effect.

The magnetic susceptibility of  $\text{Ho}_2\text{Cu}(\text{TeO}_3)_2(\text{SO}_4)_2$  was measured in the temperature range of 1.8–300 K with an applied direct-current (DC) magnetic field of 1000 Oe. The plots of  $\chi_M T$  and  $1/\chi_M$  versus temperature for  $\text{Ho}_2\text{Cu}(\text{TeO}_3)_2(\text{SO}_4)_2$  are given in Figure 5, panels a and b,

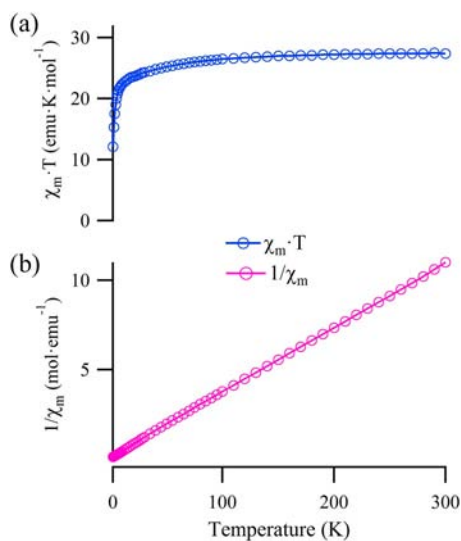


**Figure 5.** Plots of (a)  $\chi_M T$  and (b)  $1/\chi_M$  versus temperature for  $\text{Ho}_2\text{Cu}(\text{TeO}_3)_2(\text{SO}_4)_2$ .

respectively. As the temperature decreases, the  $\chi_M T$  value remains essentially constant down to 200 K. The  $\chi_M T$  value decreases gradually with the decreasing temperature and drops abruptly near 10 K, which could be attributed to the depopulation of the Stark levels of the  $\text{Ho}^{\text{III}}$  ion at low temperature.<sup>1c</sup> The susceptibility data were least-squares fit to  $1/\chi_M = (T - \theta)/C$ , where  $C$  is the Curie constant,  $\theta$  is the Weiss constant. The refined parameters corresponding to the best fit of the data in the temperature range of 50–300 K are  $C = 28.01 \text{ emu}\cdot\text{K}\cdot\text{mol}^{-1}$  and Weiss constant of  $\theta = -5.69 \text{ K}$  (Figure 4c). The Curie constant was used to calculate the effective magnetic moment by following  $\mu_{\text{eff}} = [(3kC)/N\mu_B^2]^{1/2}$ , where  $N$  is Avogadro's number and  $k$  is the Boltzmann constant, and thus  $\mu_{\text{eff}} = 14.97 \mu_B$ . The observed  $\mu_{\text{eff}}$  value has a good agreement with the calculated value of  $15.09 \mu_B$ , as

expected for two  $\text{Ho}^{\text{III}}$  and one  $\text{Cu}^{\text{II}}$  ions for the corresponding ground states  $^5\text{I}_8$  and  $^2\text{D}_{5/2}$ , respectively.<sup>19</sup>

## CONCLUSION

In conclusion,  $\text{Ho}_2\text{Cu}(\text{TeO}_3)_2(\text{SO}_4)_2$  provides a rare example of an inorganic 3d–4f hetero-bimetallic compound containing mixed anions.  $\text{Ho}_2\text{Cu}(\text{TeO}_3)_2(\text{SO}_4)_2$  exhibits two different optical transitions: a reversible thermochromic transition approximately at 100 K and changes in color under different lighting sources, the Alexandrite effect. X-ray crystal structure analyses reveals that changes of the  $\text{Cu}^{\text{II}}$  coordination geometry result in a more pronounced Jahn–Teller effect at low temperatures. However, the thermochromic transition is likely a result of a combination of changes in the absorption features of  $\text{Ho}^{\text{III}}$  and  $\text{Cu}^{\text{II}}$ .

## ASSOCIATED CONTENT

### Supporting Information

X-ray crystallographic files in CIF, video of thermochromic transition (as an mp4 file in a zip file), Figure S1, crystal image of  $\text{Ho}_2\text{Cu}(\text{TeO}_3)_2(\text{SO}_4)_2$ , table of crystallographic data, and table for selected bond distances are provided. This material is available free of charge via the Internet at <http://pubs.acs.org>.

## AUTHOR INFORMATION

### Corresponding Author

\*E-mail: [albrecht-schmitt@chem.fsu.edu](mailto:albrecht-schmitt@chem.fsu.edu).

### Notes

The authors declare no competing financial interest.

## ACKNOWLEDGMENTS

This work was supported by a Chinese Scholarship Council Graduate Fellowship to J.L. Additional support was also provided as part of the Materials Science of Actinides, an Energy Frontier Research Center funded by the U.S. Department of Energy, Office of Science, Office of Basic Energy Sciences under Award Number DE-SC0001089.

## REFERENCES

- (1) (a) Zhao, B.; Cheng, P.; Chen, X.; Cheng, C.; Shi, W.; Liao, D.; Yan, S.; Jiang, Z. *J. Am. Chem. Soc.* **2004**, *126*, 3012–3013. (b) Volklinger, C.; Henry, N.; Grandjean, S.; Loiseau, T. *J. Am. Chem. Soc.* **2012**, *134*, 1275–1283. (c) Peng, J.-B.; Zhang, Q.-C.; Kong, X.-J.; Zheng, Y.-Z.; Ren, Y.-P.; Long, L.-S.; Huang, R.-B.; Zheng, L.-S.; Zheng, Z. *J. Am. Chem. Soc.* **2012**, *134*, 3314–3317. (d) Osa, S.; Kido, T.; Matsumoto, N.; Re, N.; Pochaba, A.; Mrozinski, J. *J. Am. Chem. Soc.* **2003**, *126*, 420–421. (e) Mori, F.; Nyui, T.; Ishida, T.; Nogami, T.; Choi, K.-Y.; Nojiri, H. *J. Am. Chem. Soc.* **2006**, *128*, 1440–1441. (f) Mishra, A.; Wernsdorfer, W.; Abboud, K. A.; Christou, G. *J. Am. Chem. Soc.* **2004**, *126*, 15648–15649. (g) Glover, P. B.; Ashton, P. R.; Childs, L. J.; Rodger, A.; Kercher, M.; Williams, R. M.; De Cola, L.; Pikramenou, Z. *J. Am. Chem. Soc.* **2003**, *125*, 9918–9919.
- (2) Sorace, L.; Benelli, C.; Gatteschi, D. *Chem. Soc. Rev.* **2011**, *40*, 3092–3104.
- (3) (a) Bunzli, J.-C. G.; Eliseeva, S. V. *Chem. Sci.* **2013**, *4*, 1939–1949. (b) Bünzli, J.-C. G. *Chem. Rev.* **2010**, *110*, 2729–2755. (c) Binnemans, K.; Grolller-Walrand, C. *Chem. Phys. Lett.* **1995**, *235*, 163–174.
- (4) (a) Morita, Y.; Suzuki, S.; Fukui, K.; Nakazawa, S.; Kitagawa, H.; Kishida, H.; Okamoto, H.; Naito, A.; Sekine, A.; Ohashi, Y.; Shiro, M.; Sasaki, K.; Shiomi, D.; Sato, K.; Takui, T.; Nakasuiji, K. *Nat. Mater.* **2008**, *7*, 48–51. (b) Kennedy, B. P.; Lever, A. B. P. *J. Am. Chem. Soc.* **1973**, *95*, 6907–6913. (c) Willett, R. D.; Haugen, J. A.; Lebsack, J.; Morrey, J. *Inorg. Chem.* **1974**, *13*, 2510–2513. (d) Setifi, F.;

Benmansour, S.; Marchivie, M.; Dupouy, G. I.; Triki, S.; Sala-Pala, J.; Salaün, J.-Y.; Gómez-García, C. J.; Pillet, S. b.; Lecomte, C.; Ruiz, E. *Inorg. Chem.* **2009**, *48*, 1269–1271. (e) Andruh, M.; Ramade, I.; Codjovi, E.; Guillou, O.; Kahn, O.; Trombe, J. C. *J. Am. Chem. Soc.* **1993**, *115*, 1822–1829.

(5) Bencini, A.; Benelli, C.; Caneschi, A.; Carlin, R. L.; Dei, A.; Gatteschi, D. *J. Am. Chem. Soc.* **1985**, *107*, 8128–8136.

(6) Mitchell, K.; Ibers, J. A. *Chem. Rev.* **2002**, *102*, 1929–1952.

(7) (a) Lin, J.; Cross, J. N.; Diwu, J.; Meredith, N. A.; Albrecht-Schmitt, T. E. *Inorg. Chem.* **2013**, *52*, 4277–4281. (b) Lin, J.; Cross, J. N.; Diwu, J.; Polinski, M. J.; Villa, E. M.; Albrecht-Schmitt, T. E. *Inorg. Chem.* **2012**, *51*, 11949–11954. (c) Lin, J.; Diwu, J.; Cross, J. N.; Villa, E. M.; Albrecht-Schmitt, T. E. *Inorg. Chem.* **2012**, *51*, 10083–10085.

(8) Mao, J.-G.; Jiang, H.-L.; Kong, F. *Inorg. Chem.* **2008**, *47*, 8498–8510.

(9) Synthesis.  $\text{Ho}_2\text{O}_3$  (1 mmol,  $\text{CuSO}_4$  (1 mmol, 0.1596 g),  $\text{TeO}_2$  (2 mmol, 0.3192 g), 1 M  $\text{H}_2\text{SO}_4$  (1 mmol, 1 mL), and 1 mL of water were loaded into a 23 mL PTFE-lined autoclave linear. The autoclave was sealed and heated to 230 °C for 3 days followed by slow cooling to room temperature at a rate of 5 °C/h. The products were washed with DI water to remove soluble solids, followed by rinsing with ethanol. The products consisted of  $\text{Ho}_2\text{Cu}(\text{TeO}_3)_2(\text{SO}_4)_2$  crystals with 90% yields.

(10) (a) Harada, J.; Fujiwara, T.; Ogawa, K. *J. Am. Chem. Soc.* **2007**, *129*, 16216–16221. (b) Roof, I. P.; Smith, M. D.; Cussen, E. J.; zur Loye, H.-C. *J. Solid State Chem.* **2009**, *182*, 295–300. (c) Wang, S.; Alekseev, E. V.; Depmeier, W.; Albrecht-Schmitt, T. E. *Inorg. Chem.* **2012**, *51*, 7–9.

(11) (a) Diwu, J.; Wang, S.; Liao, Z.; Burns, P. C.; Albrecht-Schmitt, T. E. *Inorg. Chem.* **2010**, *49*, 10074–10080. (b) Diwu, J.; Nelson, A.-G. D.; Wang, S.; Campana, C. F.; Albrecht-Schmitt, T. E. *Inorg. Chem.* **2010**, *49*, 3337–3342. (c) Cross, J. N.; Villa, E. M.; Wang, S.; Diwu, J.; Polinski, M. J.; Albrecht-Schmitt, T. E. *Inorg. Chem.* **2012**, *51*, 8419–8424. (d) Diwu, J.; Good, J. J.; Di, S. V. H.; Albrecht-Schmitt, T. E. *Eur. J. Inorg. Chem.* **2011**, 1374–1377. (e) Diwu, J.; Nelson, A.-G. D.; Albrecht-Schmitt, T. E. *Comments Inorg. Chem.* **2010**, *31*, 46–62. (f) Wang, S.; Villa, E. M.; Diwu, J.; Alekseev, E. V.; Depmeier, W.; Albrecht-Schmitt, T. E. *Inorg. Chem.* **2011**, *50*, 2527–2533. (g) Sykora, R. E.; Deakin, L.; Mar, A.; Skanthakumar, S.; Soderholm, L.; Albrecht-Schmitt, T. E. *Chem. Mater.* **2004**, *16*, 1343–1349. (h) Salvadó, M. A.; Pertierra, P.; Trobajo, C.; García, J. R. *J. Am. Chem. Soc.* **2007**, *129*, 10970–10971. (i) Mihalcea, I.; Henry, N.; Clavier, N.; Dacheux, N.; Loiseau, T. *Inorg. Chem.* **2011**, *50*, 6243–6249. (j) Henry, N.; Lagrenée, M.; Loiseau, T.; Clavier, N.; Dacheux, N.; Abraham, F. *Inorg. Chem. Commun.* **2011**, *14*, 429–432.

(12) Gorden, A. E. V.; Xu, J.; Raymond, K. N.; Durbin, P. *Chem. Rev.* **2003**, *103*, 4207–4282.

(13) (a) Kim, T. H.; Shin, Y. W.; Jung, J. H.; Kim, J. S.; Kim, J. *Angew. Chem., Int. Ed.* **2008**, *47*, 685–688. (b) Khrustalev, V. N.; Kostenko, S. O.; Buzin, M. I.; Korlyukov, A. A.; Zubavichus, Y. V.; Kurykin, M. A.; Antipin, M. Y. *Inorg. Chem.* **2012**, *51*, 10590–10602.

(14) Perruchas, S.; Tard, C.; Le Goff, X. F.; Fargues, A.; Garcia, A.; Kahlal, S.; Saillard, J.-Y.; Gacoin, T.; Boilot, J.-P. *Inorg. Chem.* **2011**, *50*, 10682–10692.

(15) Krober, J.; Codjovi, E.; Kahn, O.; Groliere, F.; Jay, C. *J. Am. Chem. Soc.* **1993**, *115*, 9810–9811.

(16) Halcrow, M. A. *Chem. Soc. Rev.* **2013**, *42*, 1784–1795.

(17) (a) Shirai, T.; Nakagaki, T.; Nakai, Y.; Sugar, J.; Ishii, K.; Mori, K. *J. Phys. Chem. Ref. Data* **1991**, *20*, 1–81. (b) Sugar, J.; Musgrove, A. *J. Phys. Chem. Ref. Data* **1990**, *19*, 527–616.

(18) (a) Carnall, W. T.; Fields, P. R.; Rajnak, K. *J. Chem. Phys.* **1968**, *49*, 4424–4442. (b) Carnall, W. T.; Fields, P. R.; Rajnak, K. *J. Chem. Phys.* **1968**, *49*, 4412–4423.

(19) Buschow, K. H. J.; De Boer, F. R. *Physics of Magnetism and Magnetic Materials*, Springer: London, 2012.